

# Salicylic acid-based poly(anhydride-ester) nerve guidance conduits: Impact of localized drug release on nerve regeneration

Yong S. Lee,<sup>1\*</sup> Jeremy Griffin,<sup>1\*</sup> Shirley N. Masand,<sup>1</sup> David I. Shreiber,<sup>1</sup> Kathryn E. Uhrich<sup>1,2</sup>

<sup>1</sup>Department of Biomedical Engineering, Rutgers University, Piscataway, New Jersey 08854

<sup>2</sup>Department of Chemistry and Chemical Biology, Rutgers University, Piscataway, New Jersey, 08854

Received 21 September 2015; revised 5 December 2015; accepted 16 December 2015

Published online 20 January 2016 in Wiley Online Library (wileyonlinelibrary.com). DOI: 10.1002/jbm.a.35630

**Abstract:** Nerve guidance conduits (NGCs) can serve as physical scaffolds aligning and supporting regenerating cells while preventing scar tissue formation that often interferes with the regeneration process. Numerous studies have focused on functionalizing NGCs with neurotrophic factors, for example, to support nerve regeneration over longer gaps, but few directly incorporate therapeutic agents. Herein, we fabricated NGCs from a polyanhydride comprised of salicylic acid (SA), a nonsteroidal anti-inflammatory drug, then performed *in vitro* and *in vivo* assays. *In vitro* studies included cytotoxicity, anti-inflammatory response, and NGC porosity measurements. To prepare for implantation, type I collagen hydrogels were used

as NGC luminal fillers to further enhance the axonal regeneration process. For the *in vivo* studies, SA-NGCs were implanted in femoral nerves of mice for 16 weeks and evaluated for functional recovery. The SA-based NGCs functioned as both a drug delivery vehicle capable of reducing inflammation and scar tissue formation because of SA release as well as a tissue scaffold that promotes peripheral nerve regeneration and functional recovery. © 2016 Wiley Periodicals, Inc. *J Biomed Mater Res Part A*: 104A: 975–982, 2016.

**Key Words:** nerve guidance conduit, salicylic acid, drug delivery, nerve regeneration, tissue engineering

**How to cite this article:** Lee YS, Griffin J, Masand SN, Shreiber DI, Uhrich KE. 2016. Salicylic acid-based poly(anhydride-ester) nerve guidance conduits: Impact of localized drug release on nerve regeneration. *J Biomed Mater Res Part A* 2016;104A:975–982.

## INTRODUCTION

Annually, 700,000 patients suffer from peripheral nerve injury (PNI) in western societies.<sup>1–3</sup> Often these injuries are a result of traumatic events and accompanied by injuries to other tissues that require comprehensive treatment.<sup>2,4</sup> Loss of sensation, severe pain, and disabilities resulting from paralyzed muscles are common PNI symptoms.<sup>5</sup> Although autologous grafts are regarded as the gold standard for treating PNI, they have drawbacks including limited availability of donor nerves, possibility of neuroma formation, and sensory function loss at the donor harvest site.<sup>6</sup> These drawbacks of autologous grafts have led to research into alternate graft sources that are not derived from biological materials, but from synthetic materials such as polymer-based nerve guidance conduits (NGCs).

NGCs fabricated from synthetic polymers have many advantages compared to NGCs fabricated from naturally derived materials such as collagen and chitosan. Synthetic polymer-based NGCs are free from immunogenic concerns and batch-to-batch variability.<sup>7,8</sup> Synthetic polymers offer additional benefits over naturally derived materials in

fabrication, as they offer better control of chemical and physical properties, such as degradation rate and porosity.<sup>9,10</sup> Commonly used synthetic polymers for NGCs include poly(lactide acid) (PLA), poly(glycolic acid) (PGA), poly(lactide-co-glycolide) (PLGA), polycaprolactone (PCL), poly(caprolactone fumarate) (PCLF), and polyurethane (PU) based on their excellent biocompatibility, biodegradable nature, and potential for modification of chemical and physical properties.<sup>6,8,9,11</sup> Synthetic polymer-based NGCs typically serve as physical scaffolds to support nerve tissue alignment and prevent scar tissue infiltration,<sup>7,12–14</sup> yet require additional components to provide more clinically relevant biological cues to promote nerve regeneration over longer injury gaps.<sup>15–18</sup>

Relative to most synthetic polymers, salicylic acid (SA)-based poly(anhydride-esters) (SA-PAEs) are unique, as they degrade into anti-inflammatory products, namely SA (Scheme 1, top row).<sup>13,19–23</sup> The SA-PAEs locally deliver SA at the implantation site upon polymer degradation to mitigate inflammation and associated outcomes such as pain, swelling and infection.<sup>13</sup> As earlier studies by Griffin et al.

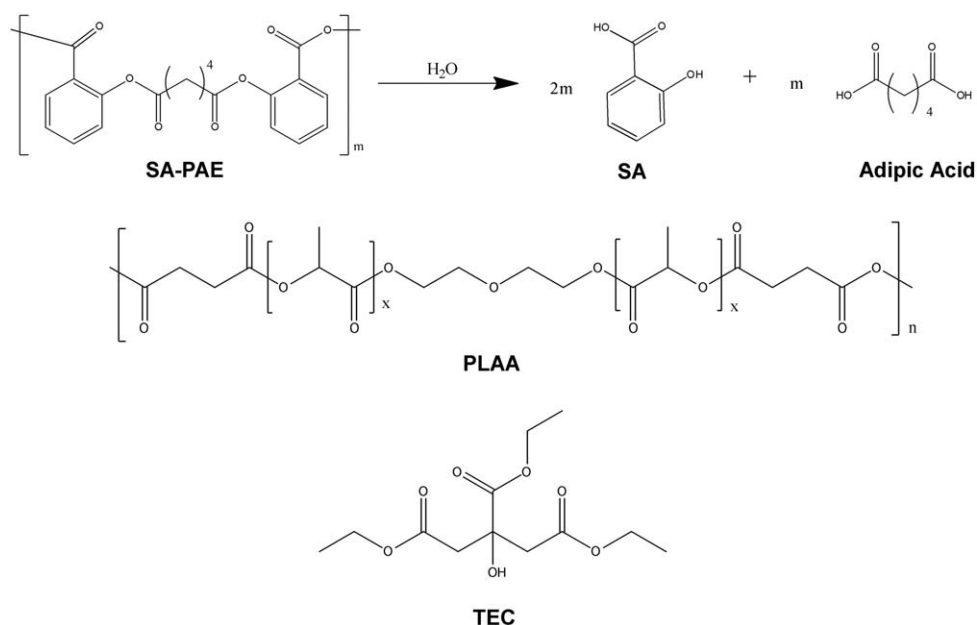
Additional Supporting Information may be found in the online version of this article.

\*These authors contributed equally to this work.

**Correspondence to:** K. E. Uhrich; e-mail: keuhrich@rci.rutgers.edu

Contract grant sponsor: National Institutes of Health; contract grant number: NIH DE 13207

Contract grant sponsor: US Army; contract grant number: W81XWH-04-2-0031



**SCHEME 1.** Chemical structures of: salicylic acid-based poly (anhydride-ester) (SA-PAE) and its degradation products, salicylic acid (SA) and adipic acid; poly(lactide anhydride) (PLAA) for blending and triethyl citrate (TEC) as a plasticizer.

have shown, the ability to locally deliver an anti-inflammatory drug via the implanted device has great potential to treat patients suffering from peripheral nerve injury without relying on systemic anti-inflammatory delivery.<sup>13</sup> Therefore, the SA-PAE-based NGCs serve the dual purpose of aiding nerve regeneration via a physical scaffold as well as reducing inflammation via localized SA release.

In this study, porous NGCs were fabricated from blends of SA-PAEs and poly(lactide anhydride) (PLAA) with additives (Scheme 1) using a dip-coating technique to generate porous structures. Other researchers have shown that NGC porosity can aid nerve regeneration by allowing the exchange of waste materials and soluble factors that affect cell viability.<sup>6,22</sup> However, hollow (that is, unfilled) NGCs have met with limited success in nerve regeneration, particularly over long gaps (>3 cm) where they are prone to fibrous tissue infiltration, collapse, and even premature resorption<sup>24</sup>. To promote nerve regeneration over long gaps, the lumens of the SA-PAE NGCs were filled with type I collagen hydrogel. Type I collagen hydrogels are known to provide a favorable environment for proliferating nerve cells.<sup>9,24–26</sup> Collagen hydrogels are also porous, restorable and can be easily added into NGCs making them suitable to be used as luminal fillers for NGCs.<sup>24</sup> An *in vivo* mouse femoral nerve model was chosen as it allows objective and sensitive functional recovery assessment.<sup>24</sup>

## MATERIALS AND METHODS

### NGC fabrication

The SA-PAEs (Scheme 1) were prepared as previously described.<sup>27</sup> In brief, PAEs were obtained via melt condensation polymerization under vacuum until the viscosity of the melt remained constant and/or solidified. The polymer had a molecular weight of 14,000 Da and glass transition

temperature ( $T_g$ ) of 40°C. Poly(lactide anhydride) (PLAA) (Scheme 1) was obtained from Bioabsorbable Therapeutics, (Menlo Park, CA).

PLAA [70 wt %] and PAEs [10 wt %] were both dissolved in dichloromethane (Sigma-Aldrich, St. Louis, MO), then triethyl citrate (Sigma-Aldrich, St. Louis, MO); 10 wt % (Scheme 1) was added to the polymer solution. Porosity and pliability of NGCs were achieved by using fine glucose powder [10 wt %] whereas TEC was utilized as a plasticizer. The fine glucose powder was prepared from glucose crystal (Sigma-Aldrich, St. Louis, MO), ground with mortar and pestle, which was then passed through sieves of known pore size (<45 μm). Teflon needles (Small Parts, Logansport, IN) of 24 gauge (outer diameter 0.7 mm) were clamped to a KSV Dip Coater (DC) [KSV Instruments Ltd., Espoo, Finland] and lowered in/out of the slurry five times at a rate of 10 mm/min [5 s in solution and 40 s out of solution].<sup>28</sup> Following five dips, the polymer-coated needles were dried in a fume hood for 48 h and then in a vacuum desiccator for 24 h. Dried polymer conduits were soaked in distilled water for 3 h to dissolve the porogen, glucose. The SA-NGCs were then dried in a vacuum desiccator for 24 h. The SA-NGCs fabricated using this dip-coating technique typically weighed ~2.5 mg ( $n = 48$ ).

### Morphology and porosity of NGCs

The SA-NGC surface morphology and microstructure was characterized using an AMRAY 1830 I scanning electron microscope (SEM). Samples were mounted on aluminum studs and sputter-coated with gold-palladium using a SCD 004 Sputter Coater (Bal-Tec, Liechtenstein). To measure the porosity, thin cross-sections (1–5 μm) of NGCs were prepared using a razor blade and mounted on aluminum studs using double-sided adhesive carbon discs. Samples were

imaged with a Zeiss EVOL5 SEM (Carl Zeiss, Peabody, MA [Coviden, North Haven, CT]) with backscatter electrons under a voltage of 20–25 kV. Cross-sectional porosity of the conduits were analyzed using ImageJ software.<sup>29</sup> A correlation between image analysis of material porosity and actual porosity values was observed, thus image threshold units were utilized to determine and differentiate the pixels of pores from non-pore pixels.<sup>30</sup> Using Otsu's thresholding, binary images were created to calculate pixel areas while minimizing the subjective aspect of thresholding grayscale images. Otsu's method optimizes the threshold for bi-level thresholding, maximizing the variance between light and dark, thereby minimizing the variance pixels associated with pores and non-pores.<sup>31,32</sup>

### ***In vitro* SA release**

Hydrolytic degradation was performed by placing segments of NGC (~7 mm in length) in 20 mL Wheaton PET plastic scintillation vials (Fisher, Fair Lawn, NJ) containing 10 mL of phosphate buffered saline (PBS, pH = 7.4; [Sigma-Aldrich, St. Louis, MO]), and incubating at 37° C with agitation at 60 rpm for 42 days (Series 25 Controlled Environment Incubator Shaker, New Brunswick Scientific Co., Edison, NJ). Degradation media (1 mL) was removed and replaced by 1 mL PBS every 24 h for the first 7 days, then once more every 7 days until the experiment was finished. The spent media was analyzed by UV ( $\lambda$  = 303 nm) with a Lamda XLS UV/vis spectrophotometer (Perkin Elmer, Waltham, MA) to determine the SA release as previously described.<sup>33</sup> A calibration curve was made from SA solutions of known concentration from the average UV data ( $n$  = 3 for each time point).

### ***In vitro* cytocompatibility**

Cell compatibility of the SA-NGC polymer blend was performed by culturing NCTC clone 929 (strain L) mouse areolar fibroblast cells (ATCC, Manassas, VA) in media containing the dissolved polymer as previously described.<sup>7</sup> The polymer was dissolved in dimethyl sulfoxide (10 mg/mL; DMSO, Sigma, St. Louis, MO) as a stock solution and serially diluted with cell culture media to two concentration (0.01 mg/mL and 0.10 mg/mL).<sup>7</sup> At a concentration of 2,000 cells per well, cells were seed into a 96-well plate (Fisher, Fair Lawn, NJ) and cultured in a solution containing the polymer, Dulbecco's Modified Eagle's Medium (DMEM, Sigma-Aldrich, St. Louis, MO), 10% fetal bovine serum (FBS, Atlanta Biologicals, Lawrenceville, GA), 1% L-glutamate (Sigma) and 1% penicillin/streptomycin (Sigma). The media containing dissolved polymer was compared to controls: DMSO-containing media; and media alone.

Cellular morphology was studied at 48, 72 and 96 h post-seeding, using 10 X original magnifications (Olympus, IX81, Center Valley, PA). Cell proliferation was determined using a CellTiter 96®Aqueous One Solution Cell Proliferation Assay (Promega, Madison, WI) and the absorbance at  $\lambda$  = 490 nm was recorded with a microplate reader (Model 680; Bio-Rad, Hercules, CA). Cell numbers were calculated based upon a standard curve established at 24 h of cell

seeding. Statistical analysis was performed with Minitab software (Minitab; State College, PA) version 15.0 for Windows. ANOVA followed by pairwise comparison with Dunnett's test (overall family error rate of 0.05) was executed with the controls being the DMSO media and the media alone.<sup>7</sup>

### ***In vitro* inflammatory response**

To assess the anti-inflammatory properties of released SA, the human acute monocytic leukemia cell line (THP-1) was differentiated into macrophage-like cells by adding phorbol 12-myristate 13-acetate (PMA; Promega) into RPMI-1640 medium (Invitrogen, Carlsbad, CA) containing 1% penicillin/streptomycin and 5% fetal bovine serum (Atlanta Biologicals). Cells were seeded at 35,000 cells/well (96-well plate) with 150  $\mu$ L medium/well. Acute inflammation was induced by the addition of lipopolysaccharide (LPS; 100 ng/mL; Sigma, St. Louis, MO) with conditioned RPMI media containing either dissolved polymer or SA. The 1.0 mM and 0.01 mM concentrations were chosen, as the relevant therapeutic SA doses used for *in vitro* assays.<sup>34,35</sup> The 400 mM and 40 mM polymer concentrations were chosen based on calculations of SAA percentage and release in SAPAE-based NGCs. Polymer-conditioned media was prepared by incubating a known mass of polymer in 10 mL of RPMI media at 37°C for 72 h. The mass loss of the original polymer was used to determine the SA concentration in the media. After 24 h of culture, the supernatant was collected and stored at –85°C. Inflammation levels were quantified by measuring tumor necrosis factor alpha (TNF- $\alpha$ ) expression, an inflammatory cytokine known to be released by THP-1 cells in response to gram-negative LPS exposure.<sup>36</sup> TNF- $\alpha$  levels were measured using a human TNF- $\alpha$  enzyme-linked immunosorbent assay (ELISA) kit (BioLegend, San Diego, CA).

THP-1 viability was determined using MTS. After 24 h of culture and complete media collection for TNF- $\alpha$  ELISA, 100  $\mu$ L of fresh RPMI medium was placed in each well with 20  $\mu$ L MTS reagent which was further incubated for 4 h. The absorbance was then recorded with a microplate reader at  $\lambda$  = 490 nm and cell numbers were calculated based upon a standard curve created 24 h after original seeding. TNF- $\alpha$  levels were normalized with THP-1 cell counts. RPMI media with LPS and PLGA with LPS were used as positive controls and RPMI media without LPS was used as a negative control.

### **NGCs preparation and surgical procedure**

NGCs were prepared as previously described.<sup>24</sup> In brief, polyethylene (PE) tubes (0.6 mm ID/1 mm OD) were used as a control group that is biocompatible, non-biodegradable, and non-bioactive. Both PE tubes and SA-NGCs were UV sterilized for 900 s using Spectrolinker 1500XL (Westbury, NY). Sterile PBS or type I collagen hydrogel was used as luminal fillers. Type I collagen hydrogels (2.0 mg/mL) were prepared as previously described.<sup>37,38</sup> Both PE tubes and SA-NGCs were incubated with type I collagen hydrogel fillers at 37°C to ensure hydrogel self-assembly.

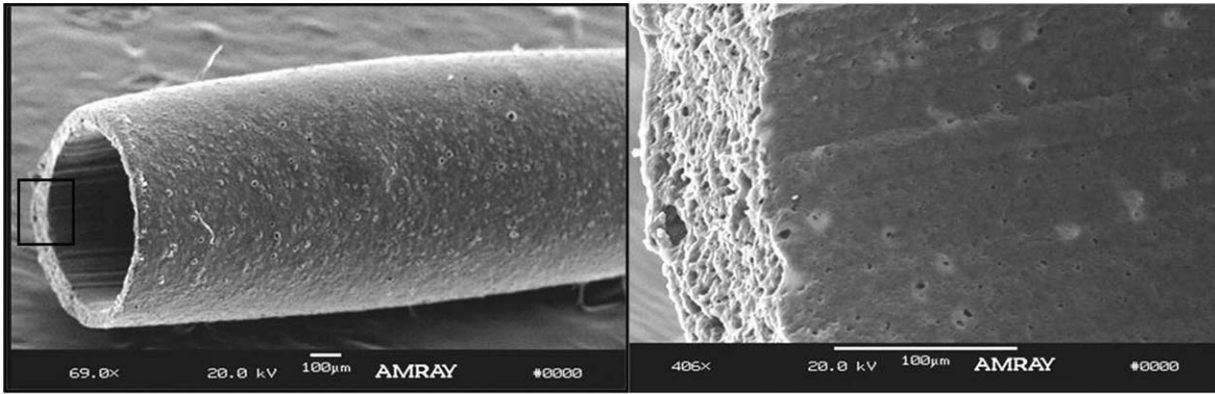


**FIGURE 1.** SEM images of the SA-NGCs: overall view at left [69X] and magnified view at right, showing the wall porosity and relatively smooth interior surface [406X]. Scale bar is 100  $\mu$ m in both images.

All animal surgeries were complied with the university standard protocols for animal handling and care. Surgical procedures were performed as previously described.<sup>24</sup> In brief, ten week-old C57/B6 female mice (Taconic Farm, Hudson, NY) were anaesthetized using mixture of ketamine (80 mg/kg) and xylazine (12 mg/mg) through intraperitoneal injections. Betadine scrub and alcohol were used to clean the surgical area prior to shaving, followed by the exposure of left femoral nerve. A 3 mm distance proximal to the bifurcation of the nerve was transected to create a 5 mm gap between the proximal and the distal stump. Either PE tubes or SA-NGCs were inserted and fixed with single epineural 10-0 nylon stitches (Ethicon, Somerville, NJ). Wound clips (Fine Science Tools, Foster City, CA) were used to close the incision on the skin, then removed from mice one week post-surgery.

### Functional recovery assessment

Injury to the femoral nerve causes a mouse to lose control of its quadriceps muscles and as a result, knee joint extension during the gait movement is limited. Using the procedure developed by Irintchev et al. functional recovery of the femoral nerve can be quantified.<sup>39</sup> In brief, mice ( $n = 6-10$ ) were trained to walk across a wooden beam (1 m) toward their home cage before the surgeries, and their gait movement filmed from the rear using a high speed camera (A602fc, Basler, Ahrensburg, Germany). The gait movements were filmed prior to injury, and at 1, 2, 4, 8, 12 and 15 weeks after nerve transection surgery was performed (See Supporting Information).

The video recordings were analyzed using single frame motion analysis software called SimiMotion (SIMI Reality Motion Systems, Unterschleissheim, Germany) to determine foot base angle (FBA). FBA is measured at the point when the sole of the left hind leg is making the contact to the beam and the contralateral leg is lifted at its highest position.<sup>24</sup> The angle is between the wooden beam and a line bisecting the left hind leg at its midpoint as shown in Figure 2. Measurement of functional recovery at various time points can be obtained using stance recovery index (RI), and calculated using the following equation:

$$RI = [(X_{\text{reinn}} - X_{\text{den}}) / (X_{\text{pre}} - X_{\text{den}})] \times 100$$

whereas  $X_{\text{reinn}}$ ,  $X_{\text{den}}$  and  $X_{\text{pre}}$  are values obtained during the period of reinnervation (reinn), the state of denervation (7 days after injury) (den), and prior to nerve injury (pre), respectively.<sup>40</sup>

### Histology

After heavy anesthesia, animals were sacrificed by perfusion through the left ventricle with 4% paraformaldehyde (Sigma-Aldrich, St. Louis, MO), and the implanted NGCs were removed. Samples for histological analysis were prepared as previously described.<sup>24</sup> In brief, samples were fixed in 4% paraformaldehyde followed by immersion in 20% sucrose-saline solution. A 2 mm segment from the middle of the regenerated nerve was sectioned and fixed with 1% osmium tetroxide solution in 0.1 M sodium cacodylate buffer then embedded in an epoxy resin (Electron Microscopy Sciences, Hatfield, PA) and sectioned into 1  $\mu$ m-thick cross-sections using Cryotome (Thermo Scientific, Waltham, MA). The samples were then counter-stained with 1% toluidine blue in 1% borax in distilled water (Electron Microscopy Sciences, Hatfield, PA), for better contrast, and imaged using 100X oil immersion objective in bright field. The captured images were then used to count the myelinated axons using ImageJ (NIH, Bethesda, MD). Degree of regeneration was calculated by dividing the area of regenerated nerve tissue by the total tissue area. The ratio of the axon-to-fiber diameter was used to calculate the g-ratio to evaluate the quality of the regenerated myelin.<sup>24</sup> The number of regenerated axons was also counted. Statistical analysis for the histological analysis was performed using R (<http://www.r-project.org/>). One-way analysis of variance (ANOVA) analysis was performed to determine the statistical significance of various data sets where  $p < 0.05$  was considered significant.

## RESULTS

### NGC porosity and inner luminal surface

Figure 1 depicts the SEM images of porous SA-NGCs. Using Ostu's threshold, SEM images revealed that SA-NGCs have



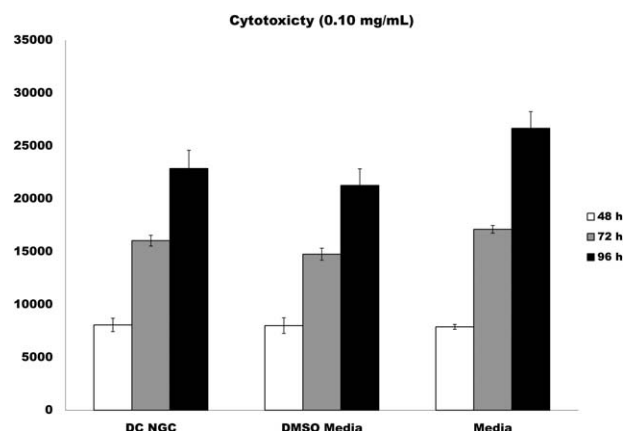


**FIGURE 2.** Cell proliferation over 4 days in culture media at concentrations of 0.10 mg polymer/mL media. No statistically significant differences were noted for the SA-NGD polymers against DMSO media, or media control were found at any of the time points using an overall family error rate of 0.05 with Dunnett's test.

porosities that are  $42 \pm 6\%$  ( $n = 12$ ) of the cross-sectional area. This aspect is relevant as porosity affects nutrient and waste transport in/out of the of the NGCs. Based on preliminary *in vivo* studies, SA-NGC pore size ranged from  $4 \sim 7 \mu\text{m}$  after 13 weeks of implantation in rats, which has been shown to aid axonal regeneration effectively.<sup>41</sup> Figure 1 shows a smooth inner luminal surface of SA-NGCs, resulting from the fabrication process in which a Teflon needle was extracted from the dried SA-NGCs.

### *In vitro* non-cytotoxicity

Increased fibroblasts number was observed for all experimental conditions over 96 h at each time point (Fig. 2). Figure 2 shows cytocompatibility data for a concentration of 0.10 mg/mL (Data for 0.01 mg/mL provided as supplemental information). No significant difference between the controls and the SA-NGCs were observed. Cultured cells display extended filopodia at all directions in all media conditions, further supporting the cytocompatibility of SA-NGCs. Cytocompatibility of the SA-NGCs was determined using a cell viability assay.

### *In vitro* salicylic acid release

The actual dose of SA released at the implantation site was determined indirectly from the average mass of the

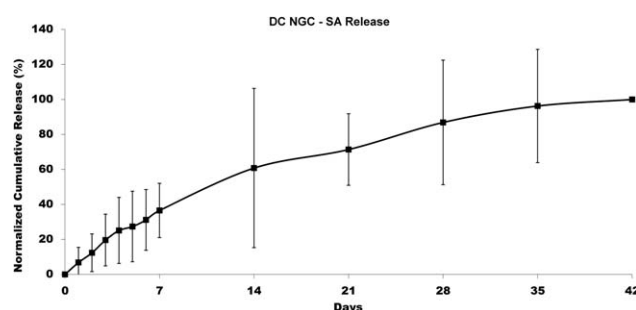


**FIGURE 3.** *In vitro* salicylic acid release profile from SA-NGCs ( $n = 3$ ).

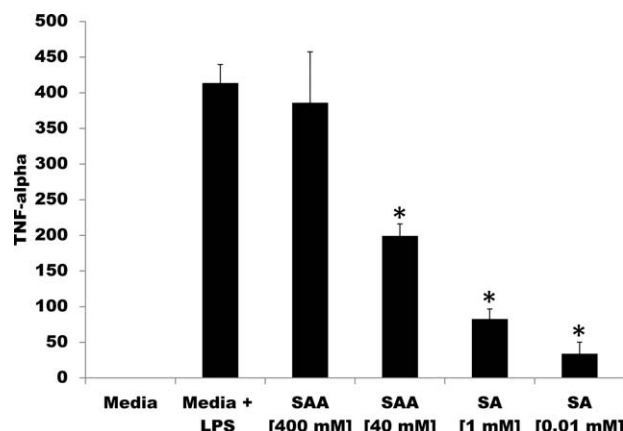


**FIGURE 4.** TNF- $\alpha$  expression over 24 h ( $n = 3$ ). Significant differences against Media LPS control indicated by \* (obtained by Dunnett's test using an overall family error rate of 0.05).

SA-NGCs and the known composition. The typical wt % of SA in the SA-PAE is  $74 \sim 75$  wt % and thus, each SA-NGCs should release  $\sim 0.18 \pm 0.01$  mg of SA. Figure 3 shows that SA is released from the SA-NGCs in a controlled and sustained manner for 42 days with no evidence of an initial burst release.

### *In vitro* anti-inflammatory response

Cumulative TNF- $\alpha$  expression of the various conditions over 24 h was examined. As indicated by pairwise comparison with Dunnett's test, a significant difference in the TNF- $\alpha$  exists between the media LPS control, SAA [40 mM], SA [1 mM], and SA [0.01 mM] after 24 h of culture (overall family error rate = 0.05) (Fig. 4). The higher concentration of SAA [400 mM] had TNF- $\alpha$  expression statistically equivalent to the media LPS, indicating a dose dependence/saturation phenomenon with SA released from the polymer.

### *In vivo* functional recovery assessment

Following injury to the femoral nerve, knee extension of the left hind leg was compromised throughout gait cycle. This motion is heavily dependent on the quadriceps with minimal contribution from other muscles, and thus serves as a good functional recovery model for regenerated nerves.<sup>24</sup> Prior to the injury, FBA was approximately  $69^\circ$  and increased to approximately  $104^\circ$  one week post-injury, indicating the loss of nerve innervation to quadriceps. After eight weeks post-injury, all groups except the saline-filled PE tube showed decreased FBA; this trend continued up to fifteen weeks post-injury. RI was normalized to the degree of functional improvement at week one to assess the functional improvement of mice during the course of 15 weeks post-surgery.<sup>24</sup> The average RI for PE NGCs including both saline and collagen fillers was 12 while the average RI for SA NGCs including both saline and collagen fillers was 22. A negative RI associated with decreased performance, suggests muscular atrophy of the animal's left hind leg due to poor nerve innervation at the target muscle. In contrast, a positive RI refers to improved gait as the nerve regenerates

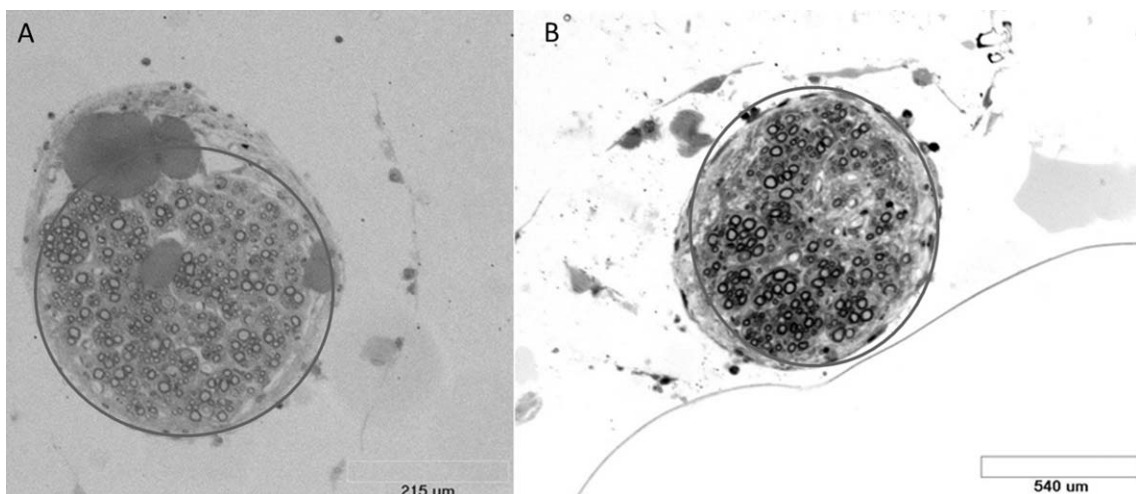


**FIGURE 5.** Histology of representative samples: (A) SA-NGC filled with saline; and (B) SA-NGC filled with native collagen. Black circles enclose the regenerated axons within the regenerated nerve. The region outside the black circles represents scar tissues.

and innervates the target muscle to support the body weight during the gait. A zero RI suggests no functional improvement due to poor nerve regeneration.

### Histological analysis

Osmium tetroxide-treated cross-sections of nerve samples showed myelinated regenerated axons in SA-NGCs with intraluminal collagen fillers (Fig. 5). As seen in Figure 5, SA-NGCs showed ample number of axons despite the small sample size. Histological analysis correlates to functional recovery (section 3.6) and morphological regeneration. For saline-filled SA-NGCs, individual mice that showed positive RI for functional assessment also showed highly regenerated axons; in contrast, animals that showed negative RI had few regenerated axons. The collagen hydrogel appears to encourage nerve regeneration and can be modified to increase myelin or axon numbers, but does not greatly increase the regeneration area - regardless of the modification. In contrast, SA-NGCs filled with intraluminal type I collagen hydrogel showed greater nerve regeneration compared to PE tubes with same interluminal filler used in the SA-NGCs.

The average number of regenerated axons in SA-NGCs was 385 which was similar to the number of the regenerated axons in our previous work<sup>24</sup>. The quality of the regenerated axons was evaluated by the g-ratio measurement. The g-ratio ranged from 0.607 to 0.717 and the average was 0.647. It has been shown that the physiologically functioning values of the g-ratio range from 0.6 to 0.8 and the lower g-ratio indicates the greater degree of myelin wrapping around the axon.<sup>24</sup>

## DISCUSSION

### NGC fabrication and porosity

NGCs serve as a physical bridge to allow regenerating nerves to reach the stump while preventing the infiltration of fibroblasts, resulting in scar tissues that may reduce the

functional recovery. Studies show that the physical properties as well as the physical dimensions of NGCs influence the nerve regeneration by preventing constriction of the regenerating nerve and avoiding early collapse.<sup>42-45</sup>. The dip-coating technique utilized in this experiment is one of the most versatile methods to readily modify the physical requirements of NGCs such as wall thickness, inner diameter, and porosity. NGC pore size must be carefully controlled to prevent escape of essential growth factors and prevent cell infiltration that may interfere with axonal elongation, yet still allow nutrient and waste exchange.<sup>6,10</sup> The smooth inner surface also enhance nerve regeneration when compared to NGCs with rough inner surface.<sup>46</sup>

### Biocompatibility of NGC and *in vitro* salicylic acid release

While the biocompatibility of SA-based PAEs have been reported,<sup>20</sup> this polymer blend has not been previously studied. Both MTS assay and cellular morphology indicate that the SA-NGCs are cytocompatible and their degradation products do not inhibit cellular proliferation. A preliminary *in vivo* study in rats exhibited no severe immunological responses (data not shown). Previous work has shown the biocompatibility of the SA-PAEs and its degradation products by culturing rat Schwann cells and primary rat dorsal root ganglia.<sup>13</sup> Based on our previous work, *in vitro* cytocompatibility, and preliminary *in vivo* study, it is unlikely that the regenerated axons will be harmed by the degradation products, SA, and adipic acid. In addition, the controlled release of SA from the SA-NGCs for a prolonged period provides benefit over systems with burst release profiles characterized by high initial concentration level above toxicity and then diminishing rapidly to ineffective concentration in body.<sup>47</sup> Furthermore, the localized release of SA is anticipated to play a role in the inhibition of scar tissue formation and TNF- $\alpha$  that could elicit the neurite outgrowth, leading to more robust regeneration.<sup>48</sup>

### ***In vivo* evaluation and histomorphological analysis**

For PNI with longer gaps, fibrin cable connections across the gap cannot be established without supportive cells and luminal fillers within the lumen of NGCs, subsequently resulting in poorly regenerated nerves.<sup>24,49</sup> When luminal fillers such as collagen hydrogels are used in conjunction with NGCs, the hydrogels replace the functions of fibrin cables and provide a favorable regeneration environment while the NGCs act as a physical bridge allowing axonal migration and regeneration.<sup>24,50</sup> In this study PE tubes filled with saline and collagen were compared to SA-NGCs filled with saline and collagen. The observed RI was better for SA-NGC based systems than PE systems. As expected the addition of collagen improved recovery. NGCs filled with type I collagen improved the RI compared to saline-filled NGCs ( $p < 0.10$ ). While intraluminal fillings are critical for axonal regeneration in longer gaps, saline-filled SA-NGCs showed improved functional recovery as well as morphological regeneration while saline-filled PE tubes showed negative functional recovery and little axonal regeneration. While further studies are required to understand the exact mechanism behind the regeneration with saline-filled SA-NGCs, we hypothesize that the SA release plays a role in improved regeneration as it should locally reduce inflammation. For example, Neumann et al. reported increased neurite outgrowth when TNF- $\alpha$  secretion was inhibited.<sup>48</sup> With the SA-based polymers, we observed reduced expression of TNF- $\alpha$  in other studies and expect the SA-NGCs to have similar influences.<sup>24</sup>

The differences between NGC composition and nerve regeneration are more apparent in Figure 6. Figure 6 shows greater percentage of nerve regeneration using SA-NGCs filled with collagen and saline compared to PE tubes filled with collagen and saline. Increased nerve regeneration percentage observed in SA-NGC groups may be due to the localized SA release, which likely suppresses inflammation and reduces the scar tissue formation to create more space for nerve growth. Our group previously reported reduced inflammation using SA based microspheres and scaffolds *in vitro* and *in vivo*,<sup>22,23</sup> SA-based microspheres significantly reduced TNF- $\alpha$  level, indicating an anti-inflammatory response. Histology revealed a reduction of inflammation *in vivo* using SA-based scaffolds when compared to PLGA scaffold. In clinical settings, reduced scar tissue formation has been reported using therapeutic dosage of SA.<sup>51,52</sup> We anticipate that the localized release of SA is playing a role in the inhibition of scar tissue formation, leading to the decrease in spatial occupancy of the scar tissue, thereby increasing the spatial distribution of regenerated tissue. Furthermore reduction of TNF- $\alpha$  has been reported to elicit neurite outgrowth, leading to more robust regeneration.<sup>48</sup>

### **CONCLUSION**

This study describes a nerve guidance conduit that is readily fabricated and has the unique benefit of locally delivering therapeutics, namely the anti-inflammatory drug, salicylic acid (SA) as the polymer degrades. Teflon needles

were dip-coated into solutions of SA-PAE and PLAA to create NGCs; this fabrication method has great potential in settings where NGCs of various dimensions are required for different types of nerve injuries. The SA-NGCs locally deliver SA at the implantation site to allow greater axonal regeneration while concurrently preventing scar tissue formation. Combined with intraluminal collagen fillers, SA-NGCs allowed a greater degree of nerve regeneration and functional movement compared to non-biodegradable PE tubes after 15 weeks post-surgery. While further studies are needed to understand the exact mechanism by which SA is improving regeneration, groups treated with saline-filled SA-NGCs showed both morphological regeneration and improved functional recovery in longer gaps that normally require luminal fillers within NGCs. This makes SA-NGCs a promising alternative to non-biodegradable PE tubes for nerve regeneration.

### **ACKNOWLEDGMENTS**

The authors would like to thank Dr. Jian Chen (W.M Keck Center for Collaborative Neuroscience, Rutgers University) for animal surgeries and Dr. Ijaz Ahmed for preparing histology samples. They also thank Prof. Freeman (Rutgers) for his review of this manuscript and Dania Agüero Davie for her editorial contributions. We confirm that all animal studies were performed accordingly to the ethical approval of all relevant agencies.

### **REFERENCES**

1. Kingham PJ, Terenghi G. Bioengineered nerve regeneration and muscle reinnervation. *J Anat* 2006;209:511–526.
2. Noble JM, Catherine A, Prasad VS, Midha R. Analysis of Upper and Lower Extremity Peripheral Nerve Injuries in a Population of Patients with Multiple Injuries. *J Trauma* 1998;45:116–122.
3. Wiberg M, Terenghi G. Will it be possible to produce peripheral nerves? *Surg Technol Int* 2003;11:303–310.
4. Scott JB, Afshari M, Kotek R, Saul JM. The promotion of axon extension *in vitro* using polymer-templated fibrin scaffolds. *Biomaterials* 2011;32:4830–4839.
5. Lundborg G, Rosen B. Hand function after nerve repair. *Acta Physiol (Oxf)*. 2007;189:207–217.
6. Jiang X, Lim SH, Mao HQ, Chew SY. Current applications and future perspectives of artificial nerve conduits. *Exp Neurol* 2010; 223:86–101.
7. Griffin J, Carbone A, Delgado-Rivera R, Meiners S, Uhrich KE. Design and evaluation of novel polyanhydride blends as nerve guidance conduits. *Acta biomaterialia* 2010;6:1917–1924.
8. Wang S, Kempen DHR, de Ruiter GCW, Cai L, Spinner RJ, Windebank AJ, et al. Molecularly engineered biodegradable polymer networks with a wide range of stiffness for bone and peripheral nerve regeneration. *Adv Funct Mater* 2015;25:2715–2724.
9. Wang S, Cai L. Polymers for fabricating nerve conduits. *Int J Polym Sci*. 2010;2010.
10. de Ruiter GC, Malesy MJ, Yaszemski MJ, Windebank AJ, Spinner RJ. Designing ideal conduits for peripheral nerve repair. *Neurosurg Focus*. 2009;26:E5.
11. Wang S, Yaszemski MJ, Knight AM, Gruetzmacher JA, Windebank AJ, Lu L. Photo-crosslinked poly(epsilon-caprolactone fumarate) networks for guided peripheral nerve regeneration: Material properties and preliminary biological evaluations. *Acta biomaterialia* 2009;5:1531–1542.
12. Cao J, Sun C, Zhao H, Xiao Z, Chen B, Gao J, et al. The use of laminin modified linear ordered collagen scaffolds loaded with laminin-binding ciliary neurotrophic factor for sciatic nerve regeneration in rats. *Biomaterials* 2011;32:3939–3948.
13. Griffin J, Delgado-Rivera R, Meiners S, Uhrich KE. Salicylic acid-derived poly(anhydride-ester) electrospun fibers designed for

- regenerating the peripheral nervous system. *J Biomed Mater Res A* 2011;97:230–242.
14. Yang XN, Jin YQ, Bi H, Wei W, Cheng J, Liu ZY, et al. Peripheral nerve repair with epimysium conduit. *Biomaterials* 2013;34:5606–5616.
  15. Sakiyama-Elbert SE, Hubbell JA. Controlled release of nerve growth factor from a heparin-containing fibrin-based cell ingrowth matrix. *J Control Release* 2000;69:149–158.
  16. Xu X, Yu H, Gao S, Ma HQ, Leong KW, Wang S. Polyphosphoester microspheres for sustained release of biologically active nerve growth factor. *Biomaterials* 2002;23:3765–3772.
  17. Kokai LE, Ghaznavi AM, Marra KG. Incorporation of double-walled microspheres into polymer nerve guides for the sustained delivery of glial cell line-derived neurotrophic factor. *Biomaterials* 2010;31:2313–2322.
  18. Kuihua Z, Chunyang W, Cunyi F, Xiumei M. Aligned SF/P(LLA-CL)-blended nanofibers encapsulating nerve growth factor for peripheral nerve regeneration. *J Biomed Mater Res A* 2013;21.
  19. Erdmann L, Macedo B, Uhrich KE. Degradable poly(anhydride ester) implants: Effects of localized salicylic acid release on bone. *Biomaterials* 2000;21:2507–2312.
  20. Schmeltzer RC, Schmalenberg KE, Uhrich KE. Synthesis and cytotoxicity of salicylate-based poly(anhydride esters). *Biomacromolecules* 2005;6:359–367.
  21. Wada K, Yu W, Elazizi M, Barakat S, Ouimet MA, Rosario-Melendez R, et al. Locally delivered salicylic acid from a poly(anhydride-ester): Impact on diabetic bone regeneration. *J Control Release* 2013;171:33–37.
  22. Mitchell A, Kim B, Cottrell J, Snyder S, Witek L, Ricci J, et al. Development of a guided bone regeneration device using salicylic acid-poly(anhydride-ester) polymers and osteoconductive scaffolds. *J Biomed Mater Res A* 2014;102:655–664.
  23. Delgado-Rivera R, Rosario-Melendez R, Yu W, Uhrich KE. Biodegradable salicylate-based poly(anhydride-ester) microspheres for controlled insulin delivery. *J Biomed Mater Res A* 2013;11.
  24. Masand SN, Chen J, Perron IJ, Hammerling BC, Loers G, Schachner M, et al. The effect of glycomimetic functionalized collagen on peripheral nerve repair. *Biomaterials* 2012;33:8353–8362.
  25. Ceballos D, Navarro X, Dubey N, Wendelschafer-Crabb G, Kennedy WR, Tranquillo RT. Magnetically aligned collagen gel filling a collagen nerve guide improves peripheral nerve regeneration. *Exp Neurol* 1999;158:290–300.
  26. Sundararaghavan HG, Monteiro GA, Firestein BL, Shreiber DI. Neurite growth in 3D collagen gels with gradients of mechanical properties. *Biotechnol Bioeng* 2009;102:632–643.
  27. Schmeltzer R, Anastasiou T, Uhrich K. Optimized synthesis of salicylate-based poly(anhydride-esters). *Polym Bull* 2003;49:441.
  28. Cai J, Peng X, Nelson KD, Eberhart R, Smith GM. Permeable guidance channels containing microfilament scaffolds enhance axon growth and maturation. *J Biomed Mater Res rA*. 2005;75:374–86.
  29. Rasband WS. Image J. US National Institutes of Health; 1997–2008.
  30. Grant PV, Vaz CM, Tomlins PE, Mikhlovskaya L, Mikhlovsky S, James S, et al. Physical characterisation of a polycaprolactone tissue scaffold. In: Blitz J, Gun'ko V, editors. *Surface Chemistry in Biomedical and Environmental Science*. 228: Springer Netherlands; 2006. p. 215–28.
  31. Kokai LE, Lin YC, Oyster NM, Marra KG. Diffusion of soluble factors through degradable polymer nerve guides: Controlling manufacturing parameters. *Acta Biomaterialia* 2009;5:2540–2550. PubMed PMID: 19369123. Epub 2009/04/17. eng.
  32. Liao PS, Chew TS, Chung PC. A fast algorithm for multilevel thresholding. *J Inf Sci Eng* 2001;17:713–727.
  33. Rosario-Melendez R, Lavelle L, Bodnar S, Halperin F, Harper I, Griffin J, et al. Stability of a salicylate-based poly(anhydride-ester) to electron beam and gamma radiation. *Polymer Degrad Stability* 2011;96:1625–1630.
  34. An Y, Liu K, Zhou Y, Liu B. Salicylate inhibits macrophage-secreted factors induced adipocyte inflammation and changes of adipokines in 3T3-L1 adipocytes. *Inflammation* 2009;32:296–303.
  35. Zu L, Jiang H, He J, Xu C, Pu S, Liu M, et al. Salicylate blocks lipolytic actions of tumor necrosis factor- $\alpha$  in primary rat adipocytes. *Mol Pharmacol*. 2008;73:215–223.
  36. Steer JH, Kroeger KM, Abraham LJ, Joyce DA. Glucocorticoids suppress tumor necrosis factor- $\alpha$  expression by human monocytic THP-1 cells by suppressing transactivation through adjacent NF- $\kappa$ B and c-Jun-activating transcription factor-2 binding sites in the promoter. *J Biol Chem*.2000;275(24):18432–18440.
  37. Masand SN, Perron IJ, Schachner M, Shreiber DI. Neural cell type-specific responses to glycomimetic functionalized collagen. *Biomaterials* 2012;33:790–797.
  38. Shreiber DI, Barocas VH, Tranquillo RT. Temporal variations in cell migration and traction during fibroblast-mediated gel compaction. *Biophys J* 2003;84:4102–4114.
  39. Irintchev A, Simova O, Eberhardt KA, Morellini F, Schachner M. Impacts of lesion severity and tyrosine kinase receptor B deficiency on functional outcome of femoral nerve injury assessed by a novel single-frame motion analysis in mice. *Eur J Neurosci*. 2005;22:802–808.
  40. Mehanna A, Mishra B, Kurschat N, Schulze C, Bian S, Loers G, et al. Polysialic acid glycomimetics promote myelination and functional recovery after peripheral nerve injury in mice. *Brain* 2009;132:1449–1462.
  41. Vleggeert-Lankamp CL, de Ruiter GC, Wolfs JF, Pego AP, van den Berg RJ, Feirabend HK, et al. Pores in synthetic nerve conduits are beneficial to regeneration. *J Biomed Mater Res A* 2007 15;80: 965–982.
  42. Oh SH, Lee JH. Fabrication and characterization of hydrophilized porous PLGA nerve guide conduits by a modified immersion precipitation method. *J Biomed Mater Res A* 2007;80:530–538.
  43. Rutkowski GE, Heath CA. Development of a bioartificial nerve graft. II. Nerve regeneration in vitro. *Biotechnol Prog* 2002;18:373–379.
  44. Ducker TB, Hayes GJ. Experimental improvements in the use of Silastic cuff for peripheral nerve repair. *J Neurosurg* 1968;28:582–587.
  45. Williams LR, Varon S. Modification of fibrin matrix formation in situ enhances nerve regeneration in silicone chambers. *J Comp Neurol* 1985;231:209–220.
  46. Aebischer P, Guenard V, Valentini RF. The morphology of regenerating peripheral nerves is modulated by the surface microgeometry of polymeric guidance channels. *Brain Res* 1990;531:211–218.
  47. Tao SL, Desai TA. Microfabricated drug delivery systems: from particles to pores. *Adv Drug Deliv Rev* 2003;55:315–328.
  48. Neumann H, Schweigreiter R, Yamashita T, Rosenkranz K, Wekerle H, Barde YA. Tumor necrosis factor inhibits neurite outgrowth and branching of hippocampal neurons by a rho-dependent mechanism. *J Neurosci* 2002;22:854–862.
  49. Pabari A, Yang SY, Mosahebi A, Seifalian AM. Recent advances in artificial nerve conduit design: strategies for the delivery of luminal fillers. *J Control Release* 2011;156:2–10.
  50. Gu X, Ding F, Yang Y, Liu J. Construction of tissue engineered nerve grafts and their application in peripheral nerve regeneration. *Prog Neurobiol* 2011;93:204–230.
  51. Danielson JR, Walter RJ. Salicylic acid may be useful in limiting scar formation. *Plast Reconstr Surg* 2004;114(5):1359–1361.
  52. Danielson JR, Walter RJ. Case studies: Use of salicylic acid (Avosil) and hydrogel (Avogel) in limiting scar formation. *J Burns Wounds* 2005;4:e6–16921411.